LETTER

https://doi.org/10.1038/s41586-019-1425-7

Modular and tunable biological feedback control using a de novo protein switch

Andrew H. Ng[1,2,3,4], Taylor H. Nguyen[1], Mariana Gómez-Schiavon[1], Galen Dods[1], Robert A. Langan[5,6,7], Scott E. Boyken[5,6], Jennifer A. Samson[2], Lucas M. Waldburger[2], John E. Dueber[2], David Baker[5,6,8] & Hana El-Samad[1,4,9]*

De novo-designed proteins[1–3] hold great promise as building blocks for synthetic circuits, and can complement the use of engineered variants of natural proteins[4–7]. One such designer protein—degronLOCKR, which is based on 'latching orthogonal cage–key proteins' (LOCKR) technology[8]—is a switch that degrades a protein of interest in vivo upon induction by a genetically encoded small peptide. Here we leverage the plug-and-play nature of degronLOCKR to implement feedback control of endogenous signalling pathways and synthetic gene circuits. We first generate synthetic negative and positive feedback in the yeast mating pathway by fusing degronLOCKR to endogenous signalling molecules, illustrating the ease with which this strategy can be used to rewire complex endogenous pathways. We next evaluate feedback control mediated by degronLOCKR on a synthetic gene circuit[9], to quantify the feedback capabilities and operational range of the feedback control circuit. The designed nature of degronLOCKR proteins enables simple and rational modifications to tune feedback behaviour in both the synthetic circuit and the mating pathway. The ability to engineer feedback control into living cells represents an important milestone in achieving the full potential of synthetic biology[10,11,12]. More broadly, this work demonstrates the large and untapped potential of de novo design of proteins for generating tools that implement complex synthetic functionalities in cells for biotechnological and therapeutic applications.

DegronLOCKR is based on LOCKR[8] technology, and consists of the designer degronSwitch and inducer protein (the 'key'). The degronSwitch is a six-helix bundle that has the cODC degron[13] embedded in the destabilized sixth helix (the 'latch'), which is occluded via intramolecular interactions with the five-helix scaffold (the 'cage'). The key can outcompete the latch for binding with the cage, which exposes the cODC degron and targets the degronSwitch and its fused cargo to the proteasome for degradation. Furthermore, the key for degronLOCKR can be genetically encoded, which ensures composability in circuit construction and distinguishes it from methods of protein degradation induced by small molecules. We capitalize on this characteristic to implement modular feedback control by directly fusing the degronSwitch to a protein of interest in a biological network and expressing the key via the transcriptional output of the network (Fig. 1a).

First, we used the degronLOCKR strategy to implement synthetic feedback in the yeast MAPK mating pathway[14] (Fig. 1b). We tested the ability of degronLOCKR to modulate pathway output by inserting the degronSwitch downstream of endogenous copies of different pathway regulators, and expressing the key using an inducible system[9] (Fig. 1c, top). Regulators in the cytoplasm or nucleus were fused to degronSwitch and targeted for degradation by using a key without or with a nuclear localization sequence (NLS), respectively (Extended Data Fig. 1). We stimulated the mating pathway with a saturating dose of α-factor in the presence and absence of the key, and monitored pathway activity with a yellow fluorescent protein (YFP) produced via the *AGA1* promoter (pAGA1-YFP-cODC[15] transcriptional reporter; p- prefix denotes promoter throughout). The degradation of different pathway regulators mediated by degronLOCKR had variable effects on the output of the mating pathway (Fig. 1c, bottom), which makes the degradation of some regulators more suitable for implementing feedback than others. Degrading cytosolic Fus3 dampened the output of the pathway whereas degrading nuclear Fus3 boosted the output, which is consistent with previous literature that implicates nuclear Fus3 as a repressor of activity of the mating pathway[16].

We implemented both synthetic negative and positive feedback control of the mating pathway by expressing nuclear key fused to a cyan fluorescent protein (CFP; key–CFP–NLS) from the mating-pathway-responsive *FIG1* promoter (pFIG1) in a strain in which either endogenous Ste12 (for negative feedback) or Fus3 (for positive feedback) is fused to the degronSwitch (Fig. 2a). In both cases, we compared the feedback strains to a strain without feedback, in which Ste12 or Fus3 was fused to degronSwitch but the key was expressed from a constitutive promoter. To test how feedback alters the behaviour of the pathway, we measured the dynamics of pAGA1-YFP-cODC reporter after stimulation with α-factor using automated flow cytometry[17] (Fig. 2b). During the time required to produce the key and activate degronLOCKR, the output of the synthetic feedback and no-feedback strains followed each other closely. After approximately two hours, the synthetic feedback activated and drove degradation of the regulator fused with degronSwitch as a function of pathway activity, causing a decrease in output for negative feedback or an increase in output for positive feedback. The synthetic negative-feedback circuit displayed larger transient overshoots for larger doses of α-factor but eventually converged to a lower steady-state output, whereas the output of the synthetic positive-feedback circuit continued to increase with large doses. This effect is likely not due to saturation of signalling, because different doses generated different transient responses (Extended Data Fig. 2).

For a more-global comparison, we measured the steady-state output dose–response of feedback and no-feedback strains as a function of α-factor. Compared to a strain with no key expression, the negative-feedback strain displayed an attenuation of the magnitude of maximum output and a decreased slope in the linear region of the dose–response; this was in contrast to the positive-feedback strain, which displayed an amplification of output and an increased slope (Fig. 2c). To confirm that this behaviour is generated by feedback, we also measured the dose–responses of strains with different levels of constitutive expression of the key[18]. The dynamic and steady-state measurements clearly demonstrate the effect of synthetic feedback and the utility of degronLOCKR as a tool for rewiring a complex endogenous signalling pathway.

We next mapped the quantitative capabilities and operational range of the degronLOCKR feedback module using a simple synthetic transcriptional cascade that consisted of two inducible synthetic transcription factors, GEM and Z3PM[9] (Fig. 3a). GEM is induced by oestradiol and

[1]Department of Biochemistry and Biophysics, University of California, San Francisco, San Francisco, CA, USA. [2]Department of Bioengineering, University of California, Berkeley, Berkeley, CA, USA. [3]The UC Berkeley–UCSF Graduate Program in Bioengineering, UC Berkeley, Berkeley, CA, USA. [4]Cell Design Initiative, University of California, San Francisco, CA, USA. [5]Department of Biochemistry, University of Washington, Seattle, WA, USA. [6]Institute for Protein Design, University of Washington, Seattle, WA, USA. [7]Graduate Program in Biological Physics, Structure, and Design, University of Washington, Seattle, WA, USA. [8]Howard Hughes Medical Institute, University of Washington, Seattle, WA, USA. [9]Chan–Zuckerberg Biohub, San Francisco, CA, USA. *e-mail: hana.el-samad@ucsf.edu

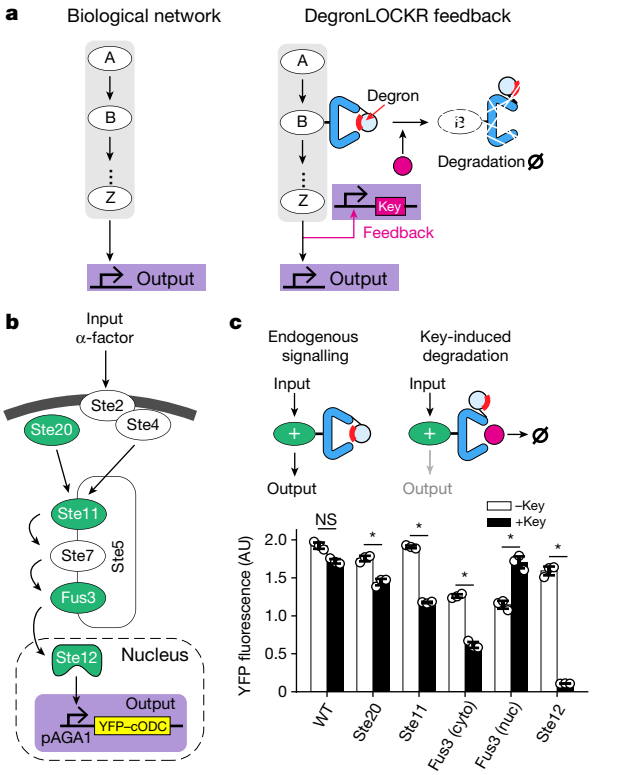

Fig. 1 | DegronLOCKR is a modular tool for controlling biological pathways. a, The degronLOCKR strategy for implementing synthetic feedback control. **b**, Simplified schematic of the yeast mating pathway, not showing endogenous feedback. Pathway is activated by addition of α-factor and signalling activity is measured using a pAGA1-YFP-cODC reporter (the promoter of *AGA1* driving YFP; the cODC degron[13] destabilizes the fluorescent reporter for measurement of dynamic pathway activity). **c**, DegronLOCKR-induced degradation of regulators of the mating pathway. The endogenous copy of the indicated protein was fused to degronSwitch and the key was expressed using a progesterone-inducible system. Cells were induced with a saturating dose of α-factor (100 nM), and pathway activity with (50 nM progesterone) and without (0 nM progesterone) the key was compared. Cyto, cytoplasm; nuc, nucleus; WT, wild type. Data represent mean ± s.d. of three biological replicates. *$P < 0.005$; NS, not significant; two-sided Student's *t*-test.

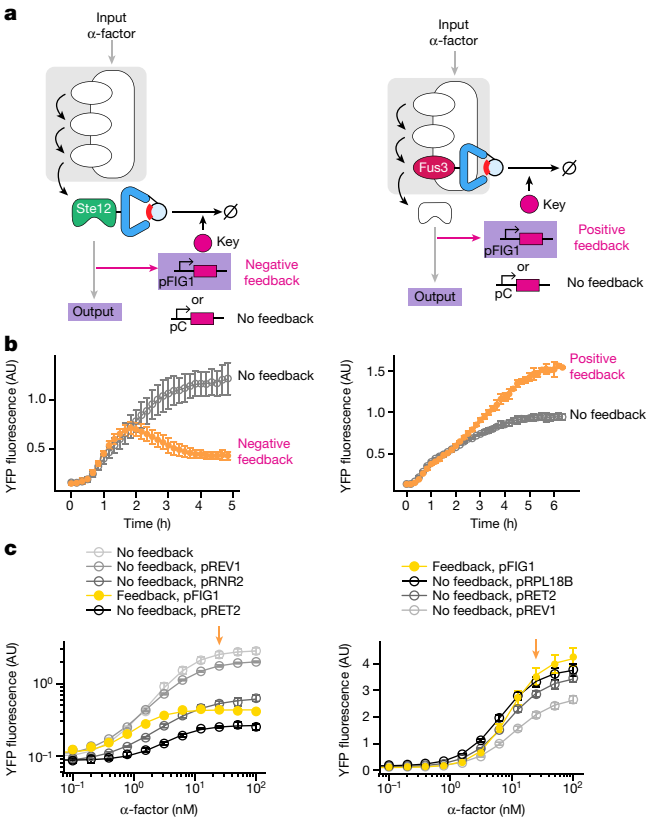

Fig. 2 | DegronLOCKR implementation of synthetic feedback on the mating pathway. a, Schematic of synthetic negative and positive feedback, in which the endogenous copy of Ste12 (left) or Fus3 (right) is fused to the degronSwitch and either a pathway-reporter *FIG1* promoter (pFIG1, synthetic feedback) or a constitutive promoter (pC, no feedback) is used to express key–CFP–NLS. All output measurements are for pAGA1-YFP-cODC. **b**, pAGA1-YFP-cODC output dynamics for synthetic negative (left) and positive (right) feedback. Synthetic feedback and no feedback (*REV1* promoter, pREV1) strains were induced at 0 h, and flow cytometry measurements (points) were performed every 10 min. Lines represent a moving average taken over three data points. **c**, Comparison of α-factor dose–response of synthetic negative (left) and positive (right) feedback. Feedback implemented using pFIG1 was compared to no-feedback strains with different levels of constitutive expression of the key. Solid lines are a Hill function fit to the data. Doses of α-factor from the experiment in **b** are indicated by arrows. Data in all panels represent mean ± s.d. of three biological replicates.

activates the *GAL1* promoter (pGAL1) to produce Z3PM, which is itself induced by progesterone and activates the synthetic pZ3 to produce the YFP-cODC reporter (pZ3-YFP-cODC). To implement feedback, we used the same modular strategy as in the mating pathway: fusing GEM to the degronSwitch and using a copy of pZ3 to express key–CFP–NLS. The addition of progesterone or induction of a photosensitive degron[19] fused to Z3PM perturbs the circuit and increases or decreases the output, respectively. A simple computational model of the circuit (Supplementary Information) predicts that feedback attenuates the effect of a progesterone disturbance by decreasing the production rate of Z3PM, which thereby compensates for an increase in Z3PM activity via a decrease in the concentration of Z3PM (Fig. 3b, Extended Data Fig. 3).

To experimentally verify these predictions, we perturbed cells that were grown to steady state with a high, medium or low step-input of progesterone, and then measured the dynamics of the pZ3-YFP-cODC output using an automated flow cytometry and an optogenetically enabled continuous-culture platform[17]. Without feedback, the step input of progesterone caused an increase in Z3PM activity and YFP expression until the output reached a new steady state that was commensurate with the disturbance. By contrast, the synthetic feedback circuit increased the expression of the key as Z3PM activity increased, which resulted in degradation of GEM and thus a decrease in the production of Z3PM. This buffering effect is visible starting two hours after the disturbance, at which time the output of the synthetic feedback circuit begins to decrease (whereas the output of the no-feedback circuit continues to climb). Because of the well-defined inputs and disturbances, adaptation after perturbation can be quantitatively assessed[20] (Methods). The feedback circuit achieved much-greater adaptation than the circuit without feedback for the positive progesterone disturbance, showcasing one of the major benefits of feedback control in attenuating disturbances (Fig. 3e).

We next tested the effect of a negative disturbance via blue-light induction of the photosensitive degron to degrade Z3PM (Fig. 3d). After an immediate decrease in YFP expression in both the synthetic feedback and no-feedback circuits, the no-feedback circuit settled to a new, lower steady state. By contrast, the feedback circuit underwent a slight overshoot, after which it recovered to a steady state that was closer to the pre-disturbance value than was observed with the no-feedback circuit. Model simulation shows that the negative disturbance pushes the output of the circuit to a lower expression level, at which the relative difference between a circuit with and without feedback will be smaller. Thus, even if feedback is actively buffering against the negative disturbance, the effect will be harder to observe (Extended Data Fig. 3,

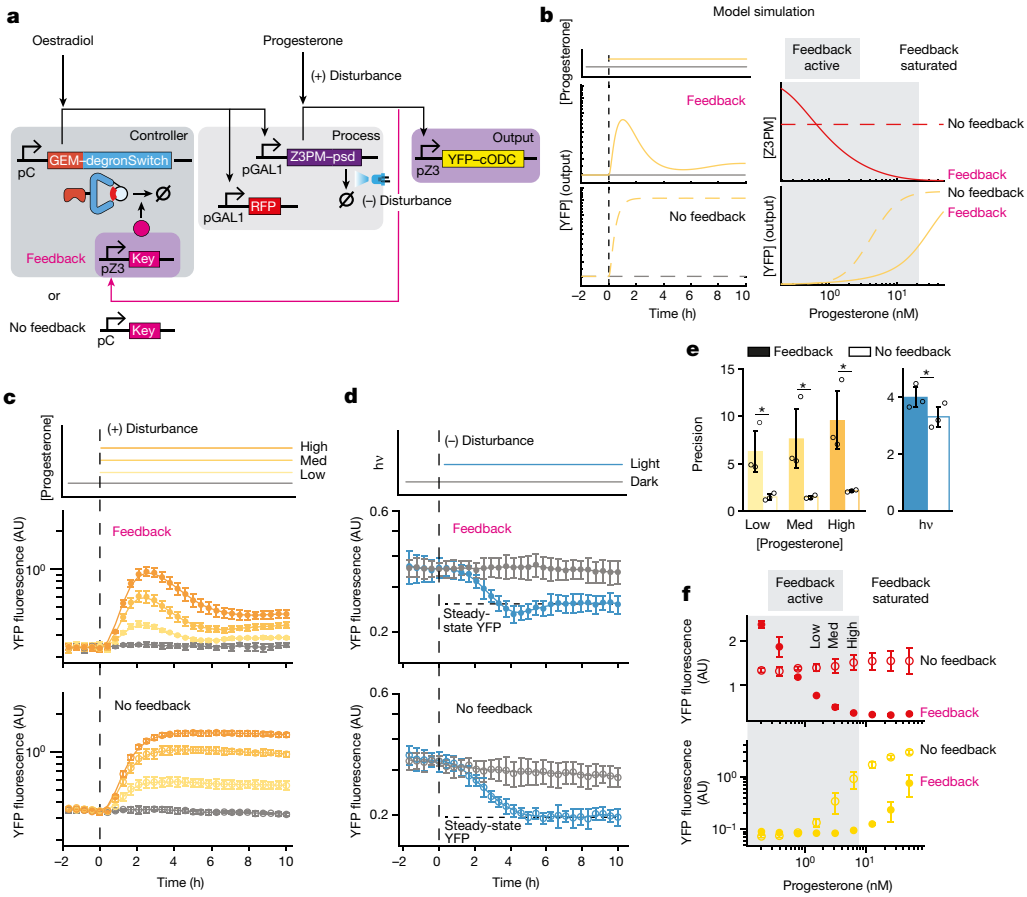

Fig. 3 | Quantifying properties of degronLOCKR feedback via control of a synthetic circuit. a, Schematic of synthetic feedback circuit. GEM–degronSwitch is expressed constitutively and is activated by oestradiol to drive expression of pGAL1-Z3PM-psd (photosensitive degron) and pGAL1-RFP. Z3PM is activated by progesterone to drive expression from the pZ3. Blue light induces degradation of Z3PM–psd. pZ3-YFP-cODC is the measured output of the circuit, and pZ3-key-CFP-NLS drives feedback in the circuit by activating degradation of GEM–degronSwitch. In the circuit with no feedback, a constitutive promoter is used to express key–CFP–NLS. **b**, Model simulation of the feedback and no-feedback circuits. The simulated dynamics that follow a progesterone disturbance (left) and steady state (right) of output indicate that feedback provides a buffer against increasing concentrations of progesterone by degrading GEM and reducing the concentration of Z3PM. **c**, Dynamic measurements of the circuit output pZ3-YFP-cODC for the synthetic feedback and no-feedback strains (key driven by the constitutive *RNR2* promoter, pRNR2-key-CFP-NLS) after a positive disturbance. Cells were grown to steady-state expression in 0.78 nM progesterone and 7.5 nM oestradiol. At 0 h, cells were either kept at the same progesterone concentration or disturbed to a final concentration of 1.56 nM (low), 3.13 nM (medium (med)) or 6.25 nM (high) progesterone. Dynamics were measured for another ten hours. **d**, Dynamic measurements of the circuit output pZ3-YFP-cODC for the synthetic feedback and no-feedback strains (key driven by the constitutive *RPL18B* promoter, pRPL18B-key-CFP-NLS) after a negative disturbance. Cells were grown to steady-state expression in 1.57 nM progesterone and 30 nM oestradiol then subjected to blue light at 0 h to activate the photosensitive degron. Dynamics were measured for another ten hours. Solid lines in **c** and **d** represent a moving average taken over three data points. **e**, Precision of the synthetic feedback versus no-feedback circuits to each of the disturbances. $*P < 0.05$; two-sided Student's *t*-test. hν, photon energy. **f**, Comparison of circuit steady-state circuit (pZ3-YFP-cODC) with and without feedback (key driven by the constitutive *RNR2* promoter; pRNR2-key-CFP-NLS) as a function of progesterone at a fixed concentration of 7.5 nM oestradiol. RFP fluorescence is a proxy for Z3PM concentration and YFP fluorescence is the output of the circuit. Progesterone doses used for positive disturbance in **c** are indicated. Data in all panels represent mean ± s.d. of three biological replicates.

Supplementary Information), which perhaps explains the difference in the performance of the circuit between positive and negative perturbations (Fig. 3f).

We next induced the feedback and no-feedback circuits with the full range of concentrations of oestradiol and progesterone, and measured both pZ3-YFP-cODC output and pGAL1-RFP (a red fluorescent protein, RFP, proxy for the activity of GEM) at steady-state (Extended Data Figs. 4, 5). At a fixed concentration of oestradiol, the output of the no-feedback circuit increases with progesterone until saturation (Fig. 3e) whereas the RFP fluorescence is insensitive to progesterone. By contrast, RFP fluorescence decreases as a function of progesterone in the synthetic-feedback circuit, which is a result of the degradation of GEM induced by degronLOCKR. This effect eventually saturates above 6.25 nM progesterone, as shown by the constant RFP expression beyond this concentration. In turn, the YFP output shows reduced sensitivity to progesterone in the region of active feedback and a marked increase when feedback is saturated. This behaviour is a unique characteristic of the feedback circuit and is not achievable by constitutively expressing different amounts of the key (Extended Data Fig. 6). Similarly, in the computational model, the feedback saturates when the complex formation between the key and degronSwitch saturates (Extended Data Fig. 3, Supplementary Information).

To enhance the utility of degronLOCKR feedback control, we next tackled the tunability of the system. The computational model predicts that tuning by changing the strength of the feedback promoter or by changing the binding affinity of the key and switch will yield a similar effect on feedback properties in most parameter regimes (Fig. 4a, Extended Data Fig. 7). To test feedback tuning via promoter strength, we used medium or weak variants of pZ3 (with four or three Z3PM binding-sites, respectively) to drive the production of the key in the feedback circuit. Measurement of the progesterone dose–response at

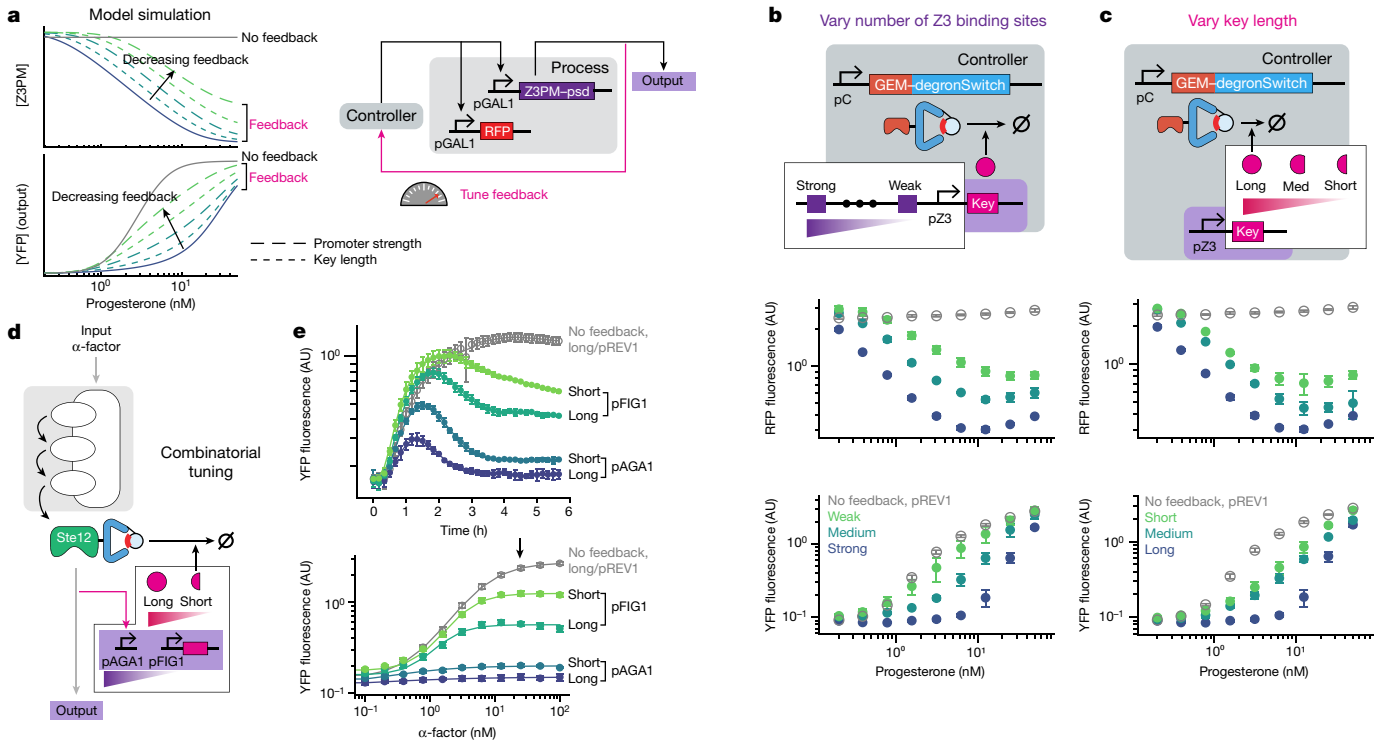

Fig. 4 | DegronLOCKR synthetic feedback is tunable. a, Exploring different tuning methods for feedback via model simulation. Z3PM and YFP steady-state output are plotted as a function of progesterone disturbance for decreasing promoter strength (dashed line) or key length (dotted line). **b**, **c**, Experimental validation of tuning. **b**, Top, tuning feedback by varying the number of Z3 binding-sites in the pZ3 with the key at a fixed length. Bottom, RFP and YFP fluorescence as a function of progesterone for strong (6×Z3PM binding-sites), medium (4×Z3PM binding-sites) and weak (3×Z3PM binding-sites) feedback strains versus the no-feedback (key driven by the constitutive *REV1* promoter; pREV1-key-CFP-NLS)) strain. **c**, Top, tuning feedback by varying the length of the key with the feedback promoter fixed at 6×Z3PM binding-sites. Bottom, RFP and YFP fluorescence as a function of progesterone for feedback strains with long (55 amino acids), medium (51 amino acids) and short (43 amino acids) keys versus no-feedback (pREV1-key-CFP-NLS)) strain. **d**, Changing promoter strength and the length of the key to tune feedback on the synthetic negative-feedback loop in the mating pathway. The pAGA1 is a stronger reporter of the mating pathway than the pFIG1. **e**, Top, dynamic measurements of pAGA1-YFP-cODC output for various feedback and no-feedback strains after stimulation with α-factor. Solid line represents a moving average taken over three data points. Bottom, α-factor dose–response of feedback strains versus a no-feedback (pREV1-key-CFP-NLS)) strain. Solid lines are a Hill function fit to the data. The dose of α-factor used in the dynamic experiment (top) is indicated by the arrow. Data in all panels represent mean ±s.d. of three biological replicates.

a fixed concentration of oestradiol demonstrated that weakening the promoter changed the dependence of the steady-state output on progesterone (Fig. 4b). As the number of binding sites was reduced, the output dose–response for the feedback circuit converged to that of the system without feedback (Extended Data Fig. 8). Similarly, decreasing the affinity of the key for the switch by truncating the full-length key by 4 (medium) or 12 (short) residues, when using the full-strength pZ3 (6×Z3PM binding-sites), led to a change in the dependence of the steady-state output on progesterone (Fig. 4c, Extended Data Fig. 8). Reducing the strength of the feedback through either one of these strategies also led to larger transients and reduced adaptation (Extended Data Fig. 9). Tuning feedback strength through the length of the key is an attractive alternative to promoter tuning and a unique strength of de novo-designed proteins.

Finally, we combinatorially tuned the synthetic negative-feedback loop in the mating pathway using both the strength of the feedback promoter and the length of the key (Fig. 4d). Replacing the pFIG1 with the stronger pAGA1 to express the key generated a pulse of expression after induction with α-factor, whereas using the pFIG1 as the feedback promoter produced sustained expression (Fig. 4e top, Extended Data Fig. 10). The size of the pulse and the steady-state output that followed it were both increased by reducing the length of the key. Reducing the length of the key when using the pFIG1 yielded a larger transient and higher steady-state output, relative to those achieved when using the pAGA1. Measurement of steady-state output as a function of the α-factor for different promoters and lengths of the key (Fig. 4e bottom, Extended Data Fig. 10) clearly demonstrates that reducing promoter strength or the length of the key increases the steady-state output of the pathway and the slope of the dose–response, which indicates reduced feedback strength. The tunability of degronLOCKR feedback makes it possible to achieve a wide range of user-specified transient and steady-state characteristics. Future advances may enable these characteristics to be computationally set during protein design.

We have presented a plug-and-play strategy for feedback control of any biological network with a transcriptional output. Previous methods for feedback control have relied on naturally occurring regulators to target specific endogenous pathways[21], which limits their modularity. In addition, the use of endogenous regulators for feedback can lead to crosstalk with other cellular pathways, which necessitates further engineering[22]. By contrast, we can directly fuse the degronSwitch to a protein of interest to generate on-target feedback on nearly any pathway of interest. The modularity of degronLOCKR extends to mammalian cells, which opens the door to a wide range of applications in the design of live cell therapeutics and in biotechnology. For example, degronLOCKR feedback control could improve therapies based on chimeric antigen receptor T cells by regulating the activity of synthetic receptors and internal signalling dynamics[23], or limit the production of toxic intermediates in metabolic pathways[24]. The feedback circuits based on degronLOCKR that we develop here open avenues for synthetic biology based on designer proteins. A toolkit of de novo-designed proteins could catalyse future applications of engineered cells in the same way that modular electronic parts have enabled the expansion of the semiconductor industry[25].

Online content

Any methods, additional references, Nature Research reporting summaries, source data, statements of data availability and associated accession codes are available at https://doi.org/10.1038/s41586-019-1425-7.

Received: 17 April 2019; Accepted: 11 June 2019;
Published online: 24 July 2019

1. Boyken, S. E. et al. De novo design of protein homo-oligomers with modular hydrogen-bond network-mediated specificity. *Science* **352**, 680–687 (2016).
2. Huang, P.-S., Boyken, S. E. & Baker, D. The coming of age of de novo protein design. *Nature* **537**, 320–327 (2016).
3. Chen, Z. et al. Programmable design of orthogonal protein heterodimers. *Nature* **565**, 106–111 (2019).
4. Andrews, L. B., Nielsen, A. A. K. & Voigt, C. A. Cellular checkpoint control using programmable sequential logic. *Science* **361**, eaap8987 (2018).
5. Toda, S., Blauch, L. R., Tang, S. K. Y., Morsut, L. & Lim, W. A. Programming self-organizing multicellular structures with synthetic cell–cell signaling. *Science* **361**, 156–162 (2018)
6. Gao, X. J., Chong, L. S., Kim, M. S. & Elowitz, M. B. Programmable protein circuits in living cells. *Science* **361**, 1252–1258 (2018).
7. Bashor, C. J. et al. Complex signal processing in synthetic gene circuits using cooperative regulatory assemblies. *Science* **364**, 593–597 (2019).
8. Langan, R. et al. De novo design of bioactive protein switches. *Nature* https://doi.org/10.1038/s41586-019-1432-8 (2019).
9. Aranda-Díaz, A., Mace, K., Zuleta, I., Harrigan, P. & El-Samad, H. Robust synthetic circuits for two-dimensional control of gene expression in yeast. *ACS Synth. Biol.* **6**, 545–554 (2017).
10. Briat, C., Gupta, A. & Khammash, M. Antithetic integral feedback ensures robust perfect adaptation in noisy biomolecular networks. *Cell Syst.* **2**, 15–26 (2016).
11. Del Vecchio, D., Dy, A. J. & Qian, Y. Control theory meets synthetic biology. *J. R. Soc. Interface* **13**, 20160380 (2016).
12. Aoki, S. K. et al. A universal biomolecular integral feedback controller for robust perfect adaptation. *Nature* **570**, 533–537 (2019).
13. Hoyt, M. A., Zhang, M. & Coffino, P. Ubiquitin-independent mechanisms of mouse ornithine decarboxylase degradation are conserved between mammalian and fungal cells. *J. Biol. Chem.* **278**, 12135–12143 (2003).
14. Bardwell, L. A walk-through of the yeast mating pheromone response pathway. *Peptides* **26**, 339–350 (2005).
15. McCullagh, E., Seshan, A., El-Samad, H. & Madhani, H. D. Coordinate control of gene expression noise and interchromosomal interactions in a MAP kinase pathway. *Nat. Cell Biol.* **12**, 954–962 (2010).
16. Chen, R. E., Patterson, J. C., Goupil, L. S. & Thorner, J. Dynamic localization of Fus3 mitogen-activated protein kinase is necessary to evoke appropriate responses and avoid cytotoxic effects. *Mol. Cell. Biol.* **30**, 4293–4307 (2010).
17. Harrigan, P., Madhani, H. D. & El-Samad, H. Real-time genetic compensation defines the dynamic demands of feedback control. *Cell* **175**, 877–886 (2018).
18. Lee, M. E., DeLoache, W. C., Cervantes, B. & Dueber, J. E. A highly characterized yeast toolkit for modular, multipart assembly. *ACS Synth. Biol.* **4**, 975–986 (2015).
19. Renicke, C., Schuster, D., Usherenko, S., Essen, L.-O. & Taxis, C. A LOV2 domain-based optogenetic tool to control protein degradation and cellular function. *Chem. Biol.* **20**, 619–626 (2013).
20. Ma, W., Trusina, A., El-Samad, H., Lim, W. A. & Tang, C. Defining network topologies that can achieve biochemical adaptation. *Cell* **138**, 760–773 (2009).
21. Bashor, C. J., Helman, N. C., Yan, S. & Lim, W. A. Using engineered scaffold interactions to reshape MAP kinase pathway signaling dynamics. *Science* **319**, 1539–1543 (2008).
22. Wei, P. et al. Bacterial virulence proteins as tools to rewire kinase pathways in yeast and immune cells. *Nature* **488**, 384–388 (2012).
23. Lim, W. A. & June, C. H. The principles of engineering immune cells to treat cancer. *Cell* **168**, 724–740 (2017).
24. Zhang, F., Carothers, J. M. & Keasling, J. D. Design of a dynamic sensor-regulator system for production of chemicals and fuels derived from fatty acids. *Nat. Biotechnol.* **30**, 354–359 (2012).
25. Moore, G. E. Progress in digital integrated electronics. In *International Electron Devices Meeting, IEEE* 11–13 (1975).

Acknowledgements We thank W. Lim, O. Weiner, and M. Lajoie for helpful discussions and P. Harrigan for assistance with hardware. This work was supported by the Defense Advanced Research Projects Agency, Contract No. HR0011-16-2-0045 to H.E.-S. The content and information does not necessarily reflect the position or the policy of the government, and no official endorsement should be inferred. H.E.-S. is a Chan-Zuckerberg investigator. A.H.N. was supported by the Department of Defense (DoD) through the National Defense Science & Engineering Graduate Fellowship (NDSEG) Program. R.A.L. was supported by Bruce and Jeannie Nordstrom, thanks to the Patty and Jimmy Barrier Gift for the Institute for Protein Design Directors Fund. S.E.B. is supported by a Career Award at the Scientific Interface from Burroughs Wellcome Fund.

Author contributions A.H.N. and H.E.-S. conceived the study and designed all experiments. T.H.N. performed dynamic experiments. A.H.N. performed all other experiments. M.G.-S., A.H.N. and H.E.-S. conceived the computational model. M.G.-S. performed all numerical simulations. G.D. contributed to plasmid and strain construction. R.A.L., S.E.B. and D.B. designed degronLOCKR and gave feedback throughout. J.A.S., L.M.W. and J.E.D. contributed to the construction of mating-pathway strains. A.H.N. and H.E.-S. wrote the manuscript and all authors edited and approved the manuscript.

Competing interests R.A.L., A.H.N., S.E.B., D.B. and H.E.-S. have filed a provisional patent application describing the design, composition and function of degronLOCKR constructs. R.A.L., A.H.N., S.E.B., D.B. and H.E.-S. have filed a provisional patent application describing the degronLOCKR-based molecular feedback circuits. D.B. and S.E.B. hold equity in Lyell Immunopharma.

Additional information
Extended data is available for this paper at https://doi.org/10.1038/s41586-019-1425-7.
Supplementary information is available for this paper at https://doi.org/10.1038/s41586-019-1425-7.
Reprints and permissions information is available at http://www.nature.com/reprints.
Correspondence and requests for materials should be addressed to H.E.
Publisher's note: Springer Nature remains neutral with regard to jurisdictional claims in published maps and institutional affiliations.

METHODS

No statistical methods were used to predetermine sample size. The experiments were not randomized and investigators were not blinded to allocation during experiments and outcome assessment.

Construction of DNA circuits. Hierarchical golden gate assembly was used to assemble plasmids for yeast strain construction using a previously published method[18]. Individual parts had their BsaI, BsmBI and NotI cut sites removed to facilitate downstream assembly and linearization. Parts were either generated via PCR or purchased as gBlocks from IDT. These parts were then assembled into transcriptional units (promoter-gene-terminator) on cassette plasmids. These cassettes were then assembled together to form multi-gene plasmids for insertion into the yeast genome.

Yeast strains and growth media. The base *Saccharomyces cerevisiae* strain used in all experiments was BY4741 (*MATa his3Δ1 leu2Δ0 met15Δ0 ura3Δ0*). All yeast cultures were grown in YPD medium (10 g/l bacto-yeast extract, 20 g/l bacto peptone and 20 g/l dextrose). Selection of auxotrophic markers (Ura3, Leu2 and/or His3) was performed on synthetic complete medium (6.7 g/l bacto-yeast nitrogen base without amino acids, 2 g/l complete supplement amino acid mix and 20 g/l dextrose). All yeast strains used in this work are listed in Supplementary Tables 1, 2.

Knockouts of FAR1 and BAR1. A modified version of BY4741 (yAHN797) was created for the mating pathway experiments with *FAR1* and *BAR1* knocked out using the CRISPR–Cas9 method, as previously outlined[18]. *FAR1* was first targeted by two single-guide (sg)RNAs designed using the Benchling biology design tool to target the open reading frame (ORF) of each gene. These sgRNAs were expressed on CEN6/ARS4 (chromosome VI centromere/autonomously replicating sequence 4) plasmids containing a Cas9 with two NLSs and a Ura3 auxotrophic marker. Repair DNA with homology to the 50 bp upstream and downstream of the ORF was generated by annealing oligonucleotides. A standard lithium acetate procedure was used to transform yeast with the plasmid containing sgRNA and Cas9 and repair DNA. The efficacy of the sgRNA was assessed by comparing the number of colonies of transformants given repair DNA with transformants that were not provided with repair DNA. Colonies were screened by colony PCR to verify the knockout, and successful clones were grown in an overnight culture of YPD. Five microlitres of overnight culture was then plated on synthetic complete medium containing 5-fluoroorotic acid (5-FOA) to counterselect the Ura3 auxotrophic marker on the CEN6/ARS4 plasmid. The knockout process was then repeated to knock out *BAR1*. Successful spacer sequences for each knockout are shown in Supplementary Table 3.

Integration of degronSwitch into the yeast genome. Oligonucleotides were designed with 80 bp of homology to target the C terminus of *STE20*, *STE11*, *MSG5*, *PTP3*, *STE12*, *DIG1*, *DIG2* and *FUS3*. Linear DNA was generated using PCR with the targeting oligonucleotides and a template of 5×GS–degronSwitch upstream of a Ura3 auxotrophic marker. Individual lithium-acetate yeast transformations were then performed to insert each of the linear DNA fragments into the parental strain yAHN797. Selection was performed on synthetic complete plates that lacked uracil, and insertions were confirmed using colony PCR. All oligonucleotides used in this study are shown in Supplementary Table 4.

Yeast cell culture and induction. Yeast strains were streaked out from a glycerol stock on SDC plates with the appropriate auxotrophic marker, or YPD plates if no auxotrophic marker was present. Individual colonies from these plates were used to inoculate a culture in YPD to grow to saturation over 12–24 h.

Testing effect of degronLOCKR on the yeast mating pathway. Saturated culture was diluted 1:500 in fresh YPD and 400 μl was aliquoted into individual wells of a 2-ml 96-well storage block (Corning) for a 3-h outgrowth at 30 °C and 900 r.p.m. in a Multitron shaker (Infors HT). The α-factor mating pheromone (Zymo Research) and progesterone (Fisher Scientific) were prepared at a 10× concentration by making the appropriate dilutions into YPD. After the 3-h outgrowth, 50 μl of α-factor and 50 μl of progesterone solution was added to the 96-well block and the block was returned to the shaker for 4 h before measurement with flow cytometry.

Induction with α-factor. Saturated culture was diluted 1:500 in fresh YPD and 450 μl was aliquoted into individual wells of a 2-ml 96-well storage block (Corning) for a 3-h outgrowth at 30 °C and 900 r.p.m. in a Multitron shaker (Infors HT). The α-factor mating pheromone was prepared at a 10× concentration by making the appropriate dilutions into YPD from a 50 μM stock solution (Zymo Research). After the 3-h outgrowth, 50 μl of α-factor solution was added to the 96-well block and the block was returned to the shaker for 4 h before measurement with flow cytometry.

Induction with oestradiol and progesterone. Saturated culture was diluted 1:500 in fresh YPD and 400 μl was aliquoted into individual wells of a 2-ml 96-well storage block (Corning) for a 3-h outgrowth at 30 °C and 900 r.p.m. in a Multitron shaker (Infors HT). Oestradiol (Sigma-Aldrich) and progesterone (Fisher Scientific) were prepared at a 10× concentration by making the appropriate dilutions into YPD from a 3.6 mM (oestradiol) and 3.2 mM (progesterone) stock solution. After the 3-h outgrowth, 50 μl of oestradiol and progesterone inducer were added to the 96-well block in the appropriate combinations and the block was returned to the shaker for 10 h before measurement with flow cytometry.

Automated flow cytometry and continuous culture system. *Hardware.* We adapted an existing automated experimental platform[17] to perform variable-concentration small-molecule induction and long-term culturing. Yeast cultures were grown in 50-ml optically clear conical tubes (Falcon) that were held in 8 custom temperature-controlled, magnetically stirred chambers. Each bioreactor was equipped with an individual blue light emitting diode (LED) that is connected to a USB-controllable LED driver (Mightex). Liquid handling was accomplished using a 14-position stream selector (VICI Cheminert) and 2 syringe pumps (Cavro XCalibur Pump, TECAN) of a BD High-Throughput Sampler (HTS). Commands to the HTS were controlled using LABVIEW 2013. This setup enabled periodic sampling and dilution of individual cultures. Each sampling period consisted of three main steps: (1) sending the sample to the flow cytometer for measurement, (2) extracting the culture and sending to waste, and (3) replenishing the culture with fresh medium at the desired concentration of hormone. Each sampling period can be designated to either induce cultures to a new, higher concentration of the hormone or to maintain the desired concentration of the hormone. Sampling frequency and dilution volume were selected to avoid saturation of culture on the basis of the duration of the experiment. For experiments longer than 6 h, a sampling frequency of 25 min and a dilution volume of 4 ml were used. For experiments shorter than six hours, continuous culturing was not performed. Instead, a single induction at 0 h was performed by extracting 2 ml of culture and replenishing with fresh medium with hormone. A sampling frequency of 10 min was used.

Yeast culture. Saturated culture was diluted 1:200, or 1:100 for mating-pathway cultures, into fresh YPD. Cultures were grown for 2 h in glass tubes at 30 °C and 250 r.p.m. in an Innova 44 shaker (New Brunswick). Cultures were then diluted to an optical density at 600 nm of 0.01 in fresh YPD, and aliquoted into individual 50-ml optically clear conical tubes (Falcon) at a total volume of 30 ml YPD. Another 1-h outgrowth was performed in bioreactors with magnetically controlled stir bars at 30 °C. All YPD medium was supplemented with 5,000 U/ml penicillin streptomycin (Thermo Fisher).

Induction with α-factor. A 1× concentration was determined by the highest-desired α-factor concentration at which to test strains (25 nM). YPD medium was prepared at two concentrations: (1) 15× α-factor concentration and (2) no α-factor. After a 1-h outgrowth in bioreactors ($t = 0$ h), induction was performed by extracting 2 ml from all cultures and replenishing with various ratios of concentrations (1) and (2) to achieve the desired concentrations. Sampling proceeded without continuous culturing.

Induction with oestradiol and progesterone for testing the rejection of positive disturbance. A 1× concentration was determined by the highest-desired hormone concentration at which to test strains (7.5 nM oestradiol and 6.5 nM progesterone). A solution of hormone and YPD medium was created at a 7.5× concentration to bring pre-induced cultures to a desired concentration in one sampling period. A second solution of hormone and YPD medium was created at a 6.7× concentration to induce cultures from their pre- to post-disturbance hormone concentrations. YPD medium was prepared at 4 concentrations of hormone: (1) 7.5× oestradiol and 7.5× progesterone, (2) 1× oestradiol and 6.7× progesterone, (3) 1× oestradiol and 1× progesterone and (4) 1× oestradiol and no progesterone. After a 1-h outgrowth in bioreactors, the first induction was performed to achieve a pre-disturbance hormone concentration by extracting 4 ml from all cultures and replenishing with concentration (1). After induction, sampling proceeded as described in 'Hardware'. All sampling periods following the induction time point included sending a sample to the cytometer for measurement, extracting 4 ml from all cultures and replenishing cultures with a mixture of concentrations (3) and (4) to maintain the desired hormone concentration. During the second induction time point ($t = 0$ h in the figures), cultures were induced to achieve a post-disturbance hormone concentration with different ratios of concentrations (2) and (4). This induction was followed by the same procedure as the first induction, except that hormone concentrations were maintained by adjusted ratios of concentrations (3) and (4).

Induction with oestradiol, progesterone and light for testing rejection of negative disturbance. A 1× concentration was determined by the highest-desired hormone concentration at which to test strains (30 nM oestradiol and 1.57 nM progesterone). A solution of hormone and YPD medium was created at a 7.5× concentration to bring pre-induced cultures to a desired concentration in one sampling period. YPD medium was prepared at three concentrations of hormone: (1) 7.5× oestradiol and 7.5× progesterone, (2) 1× oestradiol and 1× progesterone and (3) no hormone. After a 1-h outgrowth in bioreactors, the first induction was performed to achieve a pre-disturbance hormone concentration by extracting 4 ml from all cultures and replenishing with concentration (1). After induction, sampling proceeded as described in 'Hardware'. All sampling periods following the induction time point included sending a sample to the cytometer for measurement, extracting 4 ml from all cultures and replenishing cultures with a mixture of concentrations (2) and (3) to maintain the desired hormone concentration. Starting at the light induction time point ($t = 0$ h in the figures), cultures were exposed to a saturating light dose (45-s on and 15-s off, with an intensity amplitude of 25 mA) for the remainder of

the experiment. Hormone concentrations were maintained throughout the entire experiment.

Induction with oestradiol and progesterone for testing synthetic tuning. A 1× concentration was determined by the highest-desired hormone concentration at which to test strains (7.5 nM oestradiol and 3.13 nM progesterone). A solution of hormone and YPD medium was created at a 7.5× concentration to bring pre-induced cultures to a desired concentration in one sampling period. YPD medium was prepared at three concentrations of hormone: (1) 7.5× oestradiol and 7.5× progesterone, (2) 1× oestradiol and 1× progesterone and (3) no hormone. After 1-h outgrowth in bioreactors ($t = 0$ h), cultures were induced. Four millilitres were first extracted from all cultures, and then replenished with different ratios of concentrations (1) and (3) to achieve desired hormone concentrations. After induction, sampling proceeded as described in 'Hardware'. All sampling periods following the induction included sending samples to the cytometer for measurement, extracting 4 ml from all cultures and replenishing cultures at their respective hormone concentrations by adjusted ratios of concentrations (2) and (3).

Flow cytometry. Analysis of the expression of fluorescent protein reporters was performed with a BD LSRII flow cytometer (BD Biosciences) equipped with a high-throughput sampler. For steady-state measurements, cultures were diluted in TE before running through the instrument to obtain an acceptable density of cells. YFP (Venus) fluorescence was measured using the FITC channel and RFP (mKate2) was measured using the PE–Texas Red channel. For steady-state measurements, 5,000-10,000 events were collected per sample. For dynamic measurements, the first 750 events of sample were discarded, and 2,000–10,000 events were collected per sample. Fluorescence values were calculated using the height measurement for the appropriate channel and normalized to cell size by dividing by side scatter (SSC-H). All analysis of flow cytometry data was performed in Python 2.7 using the package FlowCytometryTools and custom scripts.

Precision calculations. Precision for a progesterone disturbance was calculated as follows:

$$\left(\frac{|\mathrm{YFP}_{\mathrm{post}}-\mathrm{YFP}_{\mathrm{pre}}|/\mathrm{YFP}_{\mathrm{pre}}}{|\mathrm{Pg}_{\mathrm{post}}-\mathrm{Pg}_{\mathrm{pre}}|/\mathrm{Pg}_{\mathrm{pre}}}\right)^{-1}$$

in which $\mathrm{YFP}_{\mathrm{post}}$ is the steady-state YFP fluorescence value after disturbance, $\mathrm{YFP}_{\mathrm{pre}}$ is the steady-state YFP fluorescence value before disturbance, $\mathrm{Pg}_{\mathrm{post}}$ is the post-disturbance progesterone concentration and $\mathrm{Pg}_{\mathrm{pre}}$ is the pre-disturbance progesterone concentration. For light disturbance, precision was calculated as follows:

$$\left(\frac{|\mathrm{YFP}_{\mathrm{post}}-\mathrm{YFP}_{\mathrm{pre}}|}{\mathrm{YFP}_{\mathrm{pre}}}\right)^{-1}$$

Hill function fitting. The mean of triplicate data from each α-factor dose–response was used to fit a Hill function of the following form:

$$F(\alpha) = F_{\mathrm{min}} + (F_{\mathrm{max}} - F_{\mathrm{min}}) \times \frac{\alpha^n}{K_{\mathrm{m}}^n + \alpha^n},$$

in which $F(\alpha)$ is the mean fluorescence, F_{min} is the basal fluorescence, F_{max} is the maximum fluorescence, K_{m} is the α-factor concentration at which half-maximal fluorescence is achieved, and n is the Hill coefficient. Fitting was performed in Python 2.7 using the Scipy package and the curve_fit function. Parameters from each fitting are reported in Supplementary Information Table 5.

Reporting summary. Further information on research design is available in the Nature Research Reporting Summary linked to this paper.

Data availability

All data that support the findings of this study are available within the Letter and its Supplementary Information. Original data that supports the findings are available from the corresponding author upon reasonable request. Plasmids that encode the synthetic controller and process are available from Addgene (plasmids 127164 and 127165).

Code availability

Code that supports the findings of this study is available at https://github.com/andrewng1023/NatureFeedbackdegronLOCKR.

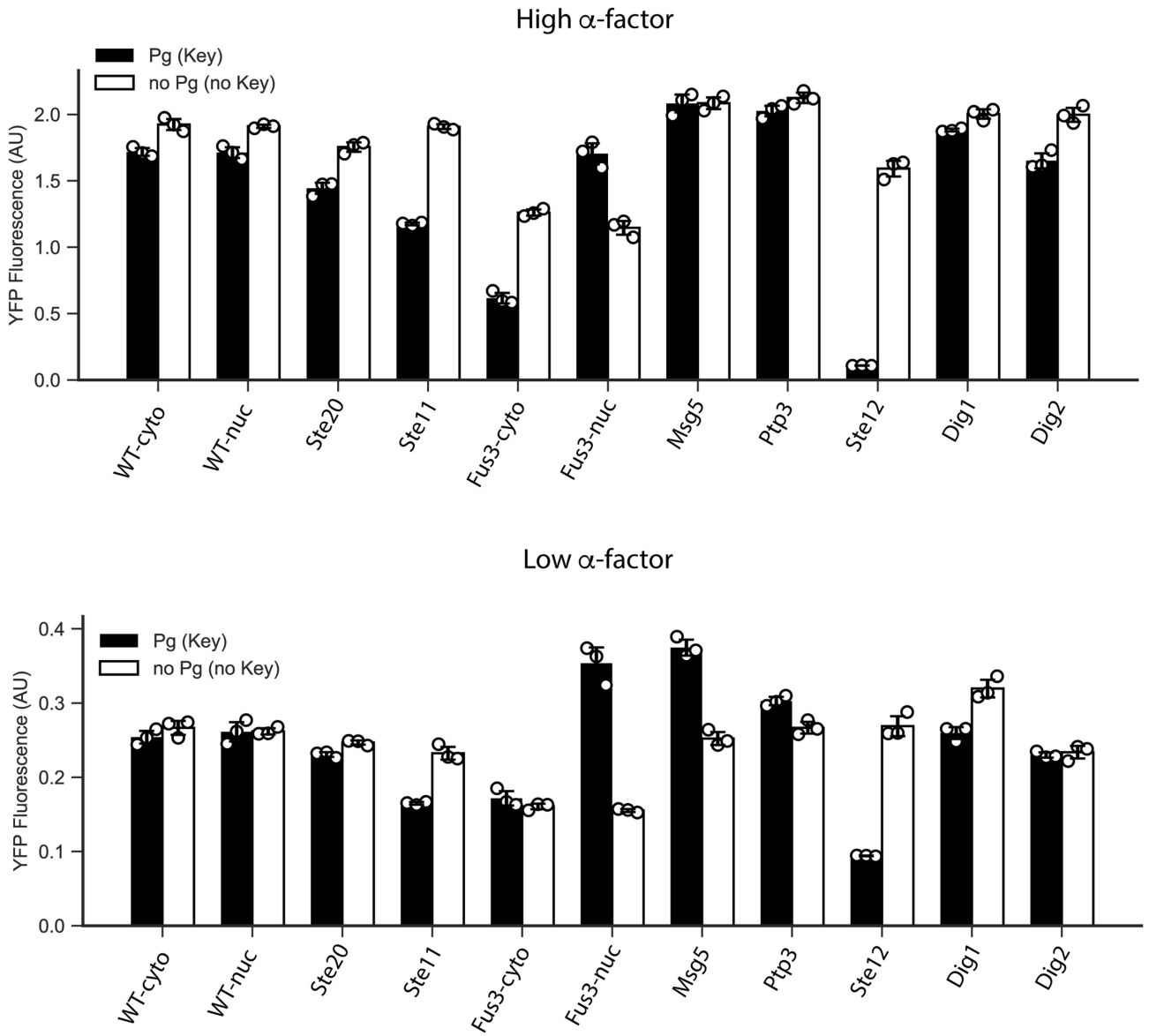

Extended Data Fig. 1 | Panel of mating-pathway regulators tested with degronLOCKR. DegronSwitch was fused to the C terminus of the endogenous copy of each regulator. The key with or without a SV40 NLS was expressed using a progesterone (Pg)-inducible system[8]. Ste20, Ste11 and Ptp3 were degraded using a cytoplasmic key (key–CFP), and Msg5, Ste12, Dig1 and Dig2 were degraded using a nuclear key (key–CFP–NLS). Fus3 was degraded using either a cytoplasmic or a nuclear key. Cells were induced with 1 nM (low) or 100 nM (high) α-factor and 50 nM or 0 nM progesterone, and grown for 4 h before YFP fluorescence was measured using a flow cytometer. Data represent mean ± s.d. of three biological replicates.

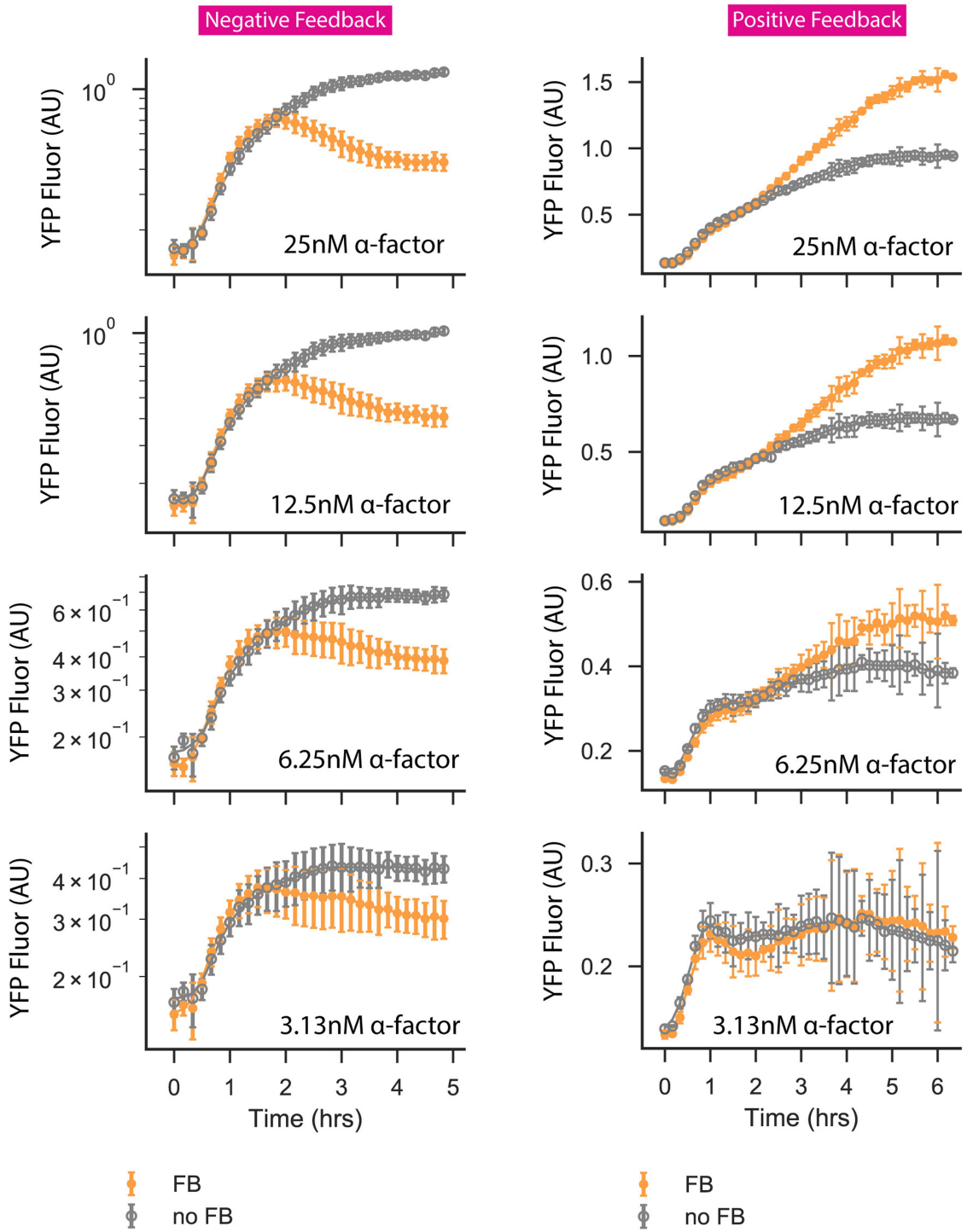

Extended Data Fig. 2 | Dynamic measurements of the mating pathway with synthetic feedback. DegronSwitch was fused to the C terminus of the endogenous copy of Ste12 (left) and Fus3 (right). Measurements of pAGA1-YFP-cODC dynamics for synthetic negative (left) and positive (right) feedback. Synthetic feedback and no-feedback (pREV1-key-CFP-NLS) strains were induced with 25, 12.5, 6.25 or 3.13 nM α-factor at 0 h, and flow cytometry measurements (points) were performed every 10 min. Points represent the mean ± s.d. of three biological replicates. Lines represent a moving average taken over three data points.

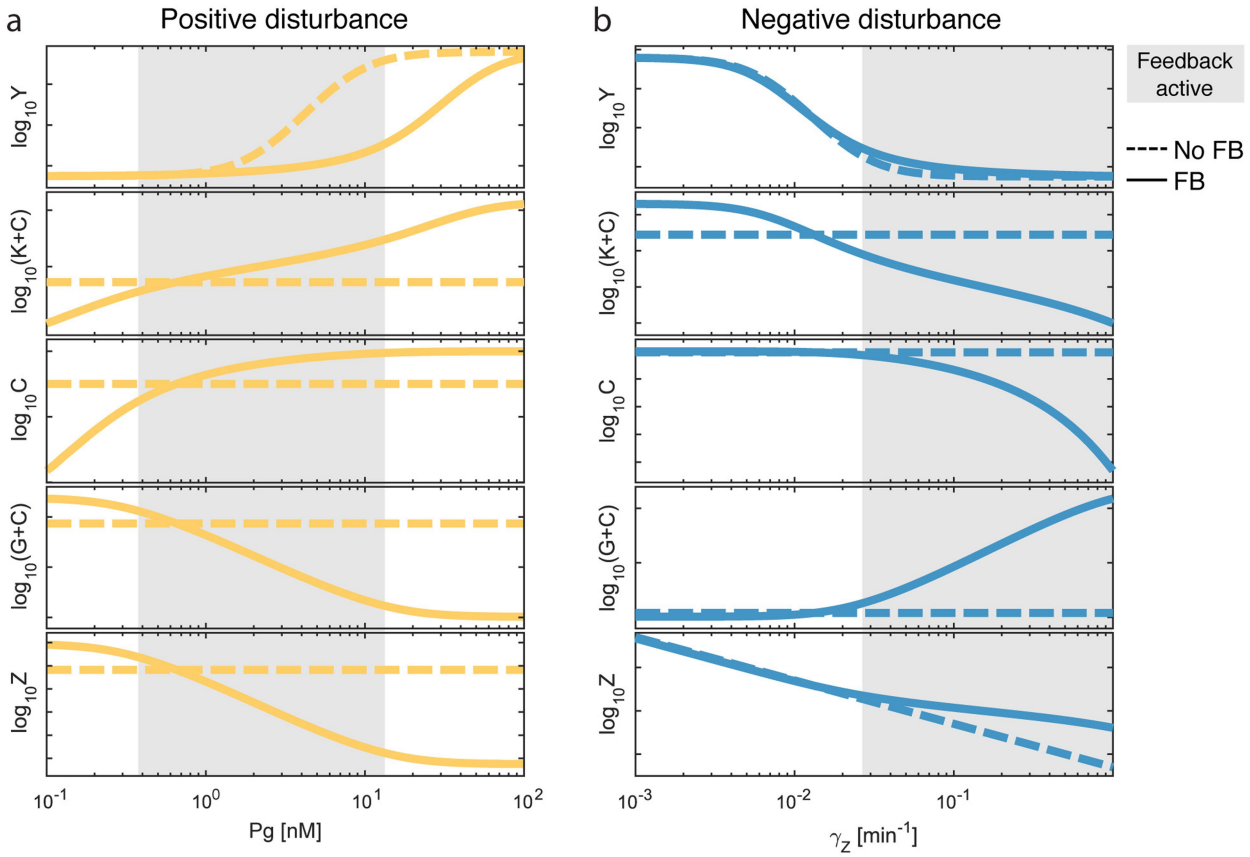

Extended Data Fig. 3 | Model analysis of synthetic transcriptional circuit with degronLOCKR feedback to probe steady-state solutions in response to positive or negative disturbances. a, **b**, Steady-state values of model variables as progesterone (**a**) or Z3PM degradation rate (γ_Z) (**b**) change (see 'Model description' in Supplementary Information). Continuous lines correspond to the feedback system (FB), and the dashed lines show an example in which the feedback has been removed (no FB; that is, $f_K = \mu_{K*}$ instead of equation (12) in Supplementary Information). The grey box delimits the area in which the feedback is considered to be 'active'. This is defined by the relative change in total GEM ($\Delta(G + C)/(G + C)$) over the relative change of the disturbance ($\Delta P/P$ for **a** or $\Delta\gamma_Z/\gamma_Z$ for **b**) being higher than 0.15. In the absence of feedback, $\Delta(G + C)$ is equal to zero for any disturbance, unless the disturbance directly affects the synthesis or degradation rate of the key or GEM. The parameters used, and definitions of variables and species, are provided in the Supplementary Information.

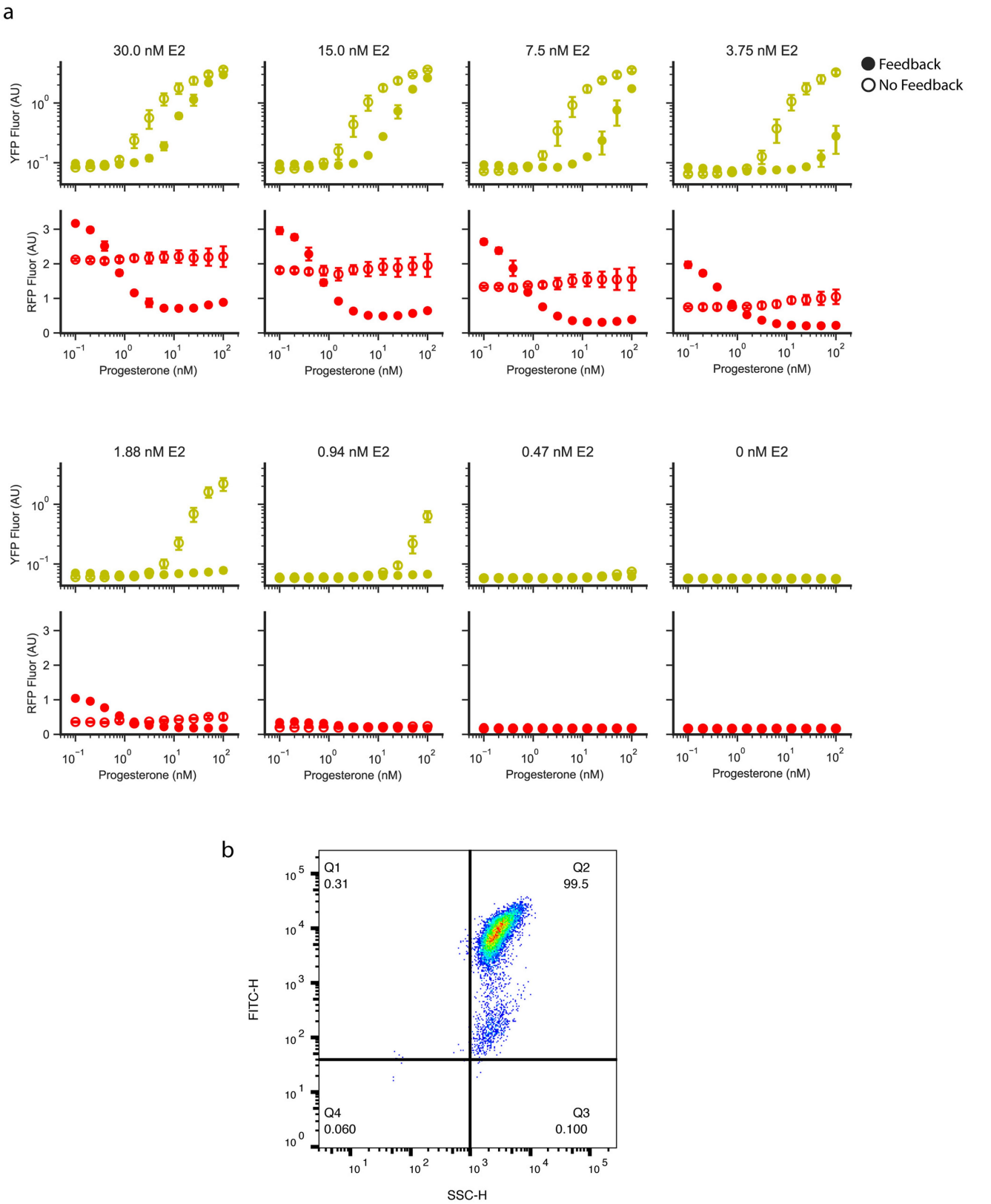

Extended Data Fig. 4 | Experimental behaviour of synthetic transcriptional circuit with degronLOCKR feedback as a function of progesterone for a fixed dose of oestradiol. a, Comparison of behaviour of the steady-state circuit (ten hours after stimulation) with and without feedback (pRNR2-key-CFP-NLS) as a function of progesterone at all concentrations of oestradiol (E2). YFP fluorescence is the output of the circuit and RFP fluorescence is a proxy for Z3PM concentration. Points represent mean ± s.d. of three biological replicates. **b**, Example of gating strategy used to generate flow cytometry data. The cells that were used are in Q2.

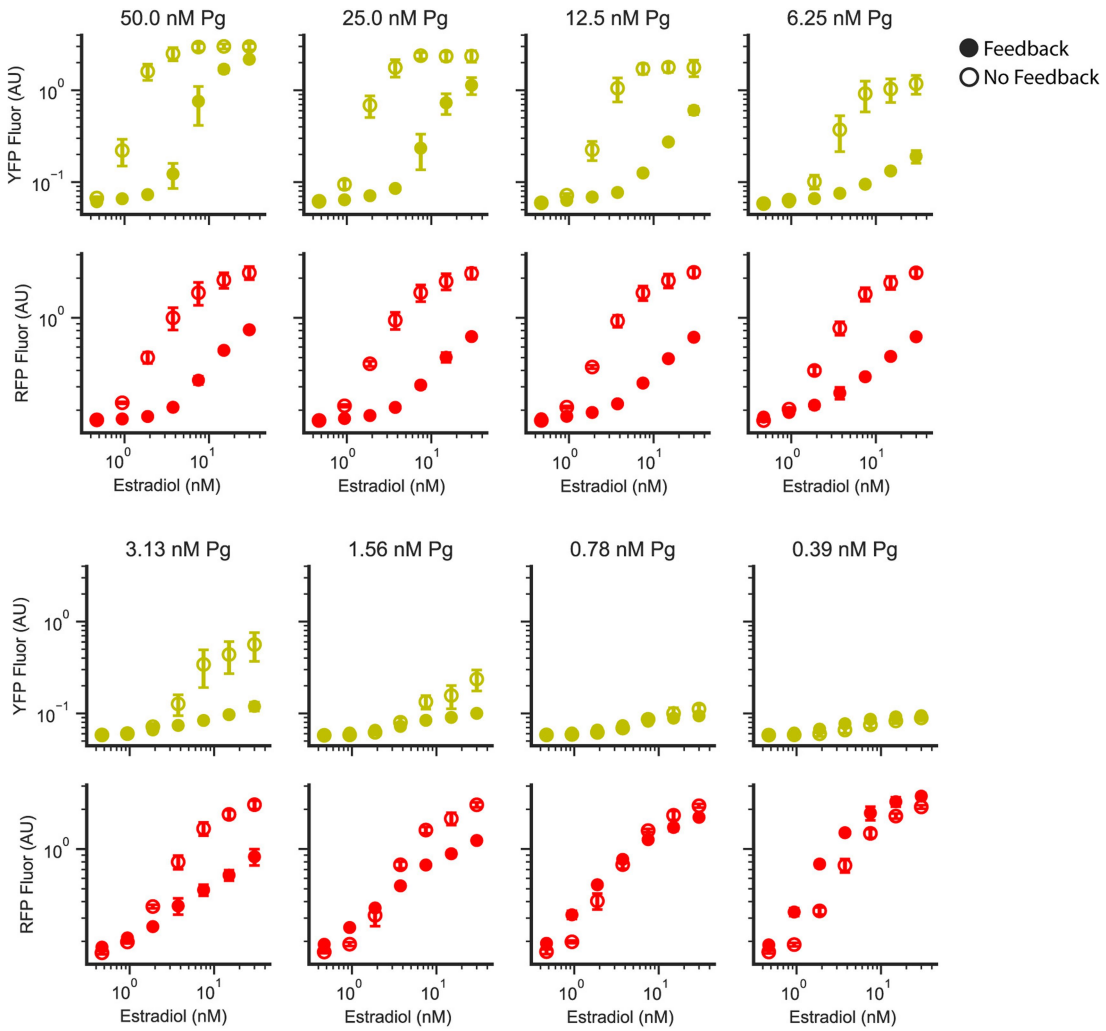

Extended Data Fig. 5 | Experimental behaviour of synthetic transcriptional circuit with degronLOCKR feedback as a function of oestradiol for a fixed dose of progesterone. Comparison of the behaviour of the steady-state circuit (ten hours after stimulation) with and without feedback (pRNR2-key-CFP-NLS) as a function of oestradiol at all concentrations of progesterone. YFP fluorescence is the output of the circuit and RFP fluorescence is a proxy for Z3PM concentration. Points represent mean ± s.d. of three biological replicates.

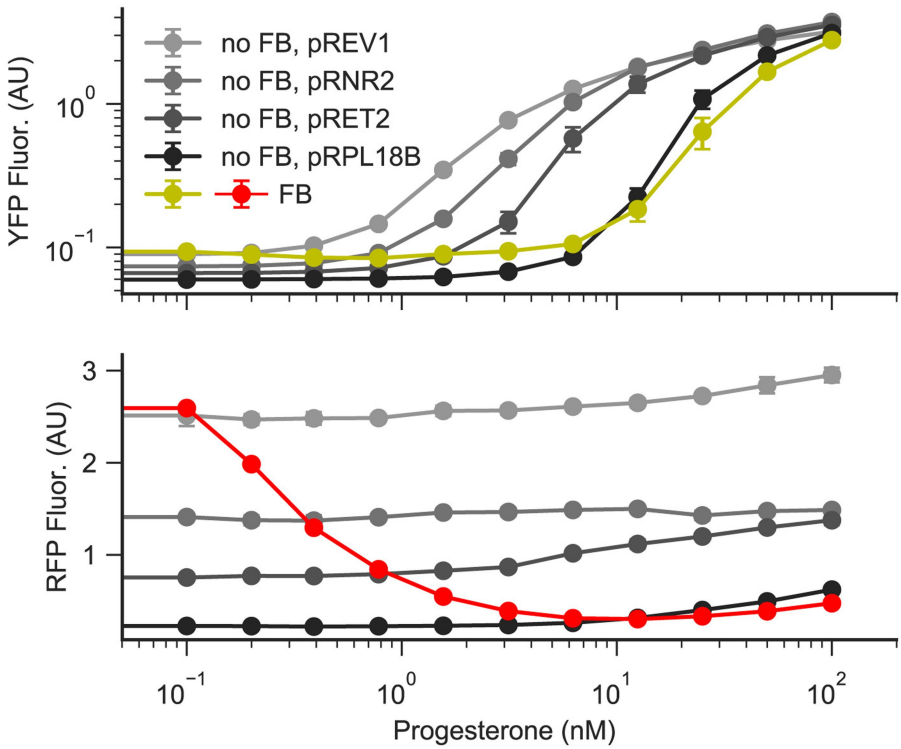

Extended Data Fig. 6 | Behaviour of synthetic transcriptional circuit with degronLOCKR feedback cannot be matched by constitutively expressing different amounts of the key. Comparison of the behaviour of the steady-state circuit (ten hours after stimulation) with feedback, and various levels of expression of the key without feedback (*REV1*, *RNR2*, *RET2* and *RPL18B* promoters), as a function of progesterone at a fixed concentration of 7.5 nM oestradiol. YFP fluorescence is the output of the circuit and RFP fluorescence is a proxy for Z3PM concentration. The yellow line in the top panel is the YFP output for the feedback circuit, and the red line in the bottom panel is the RFP output for the feedback circuit. Points represent mean ± s.d. of three biological replicates. Data points are connected by lines to guide the eye.

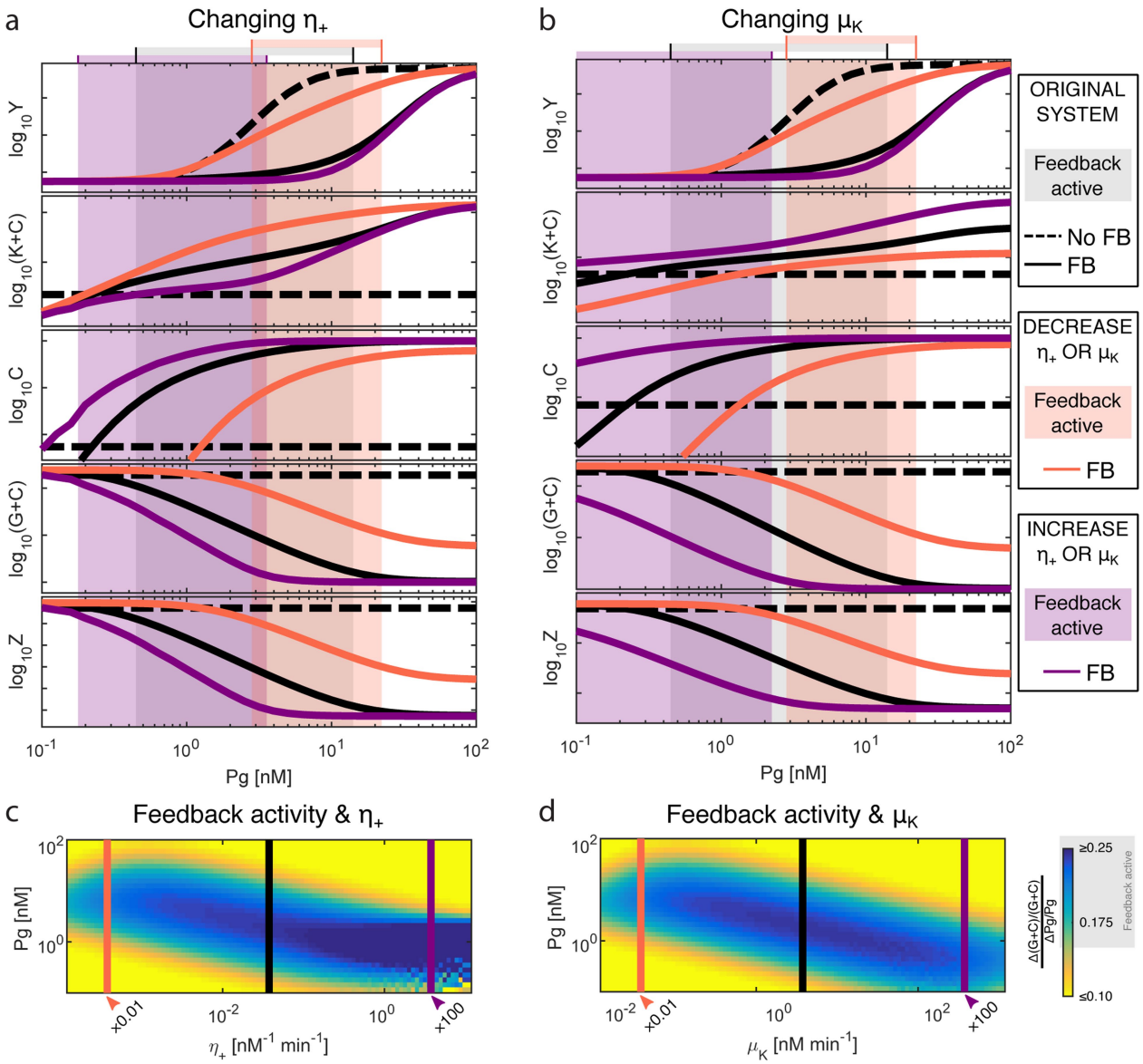

Extended Data Fig. 7 | Model analysis of synthetic transcriptional circuit with degronLOCKR feedback to probe the effect of changing η_+ or μ_K on steady state solution & feedback activity. a, **b**, Steady values as progesterone changes according to the model (see 'Model description' in Supplementary Information). Continuous lines correspond to model simulation of the feedback system, and the dashed line shows an example in which the feedback has been removed ($f_K = \mu_{K^*}$ instead of equation (12) in Supplementary Information). The effect of decreasing (×0.01) or increasing (×100) η_+ (**a**) or μ_K (**b**) are shown in orange or purple, respectively. The shadow boxes delimit the area in which the feedback is considered to be active ($((\Delta(G+C)/(G+C))/(\Delta P/P) > 0.15$) for each case. Grey, original parameter set; orange, decreasing η_+ (**a**) or μ_K (**b**); purple, increasing η_+ (**a**) or μ_K (**b**). **c**, **d**, Range of feedback activity for progesterone disturbances, and how this changes as η_+ (**c**) or μ_K (**d**) varies. See colour bar on the right for precision metric. The colours of the vertical lines in c and d correspond to the cases shown in a and b, respectively.

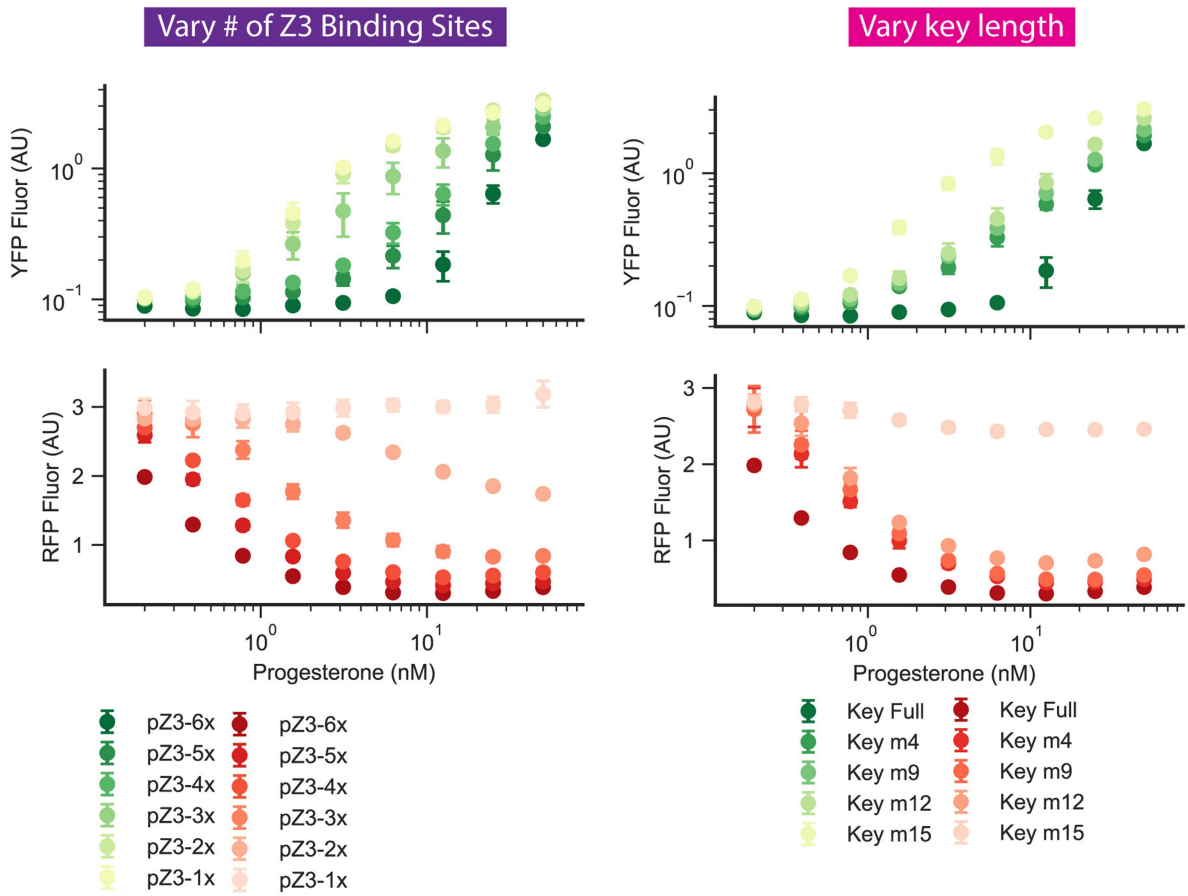

Extended Data Fig. 8 | Changing the promoter strength or length of the key in experiments modulates the steady-state properties for the synthetic transcriptional circuit with degronLOCKR feedback. Comparison of the behaviour of the steady-state circuit (ten hours after stimulation) for various levels of feedback as a function of progesterone, at a fixed concentration of 7.5 nM oestradiol. Left, tuning via changing the strength of the feedback promoter. x, number of Z3 binding sites. Right, tuning via changing the length of the key. m, number of residues removed from the C- terminus of the key. YFP fluorescence (top panels) is the output of the circuit, RFP fluorescence (bottom panels) is a proxy for Z3PM concentration. Points represent mean ± s.d. of three biological replicates.

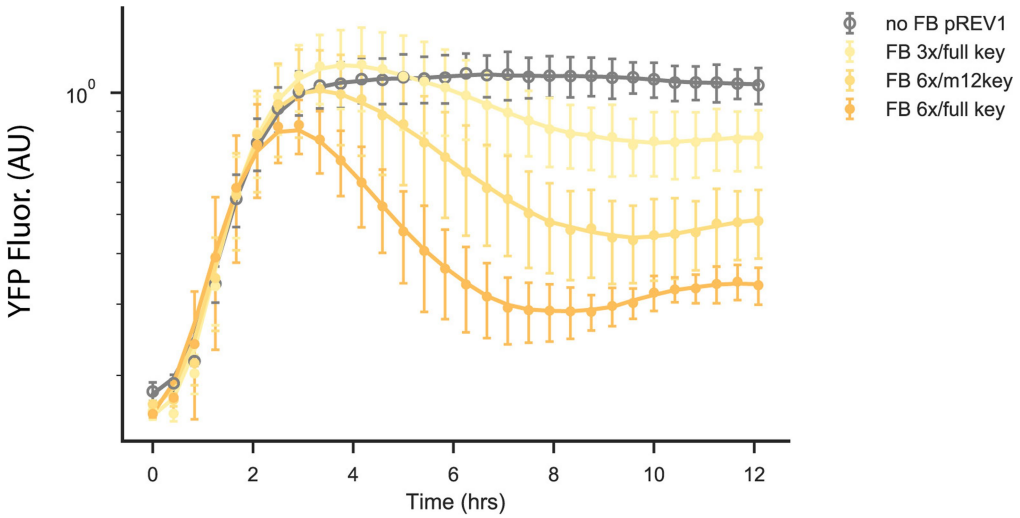

Extended Data Fig. 9 | Changing the length of the key in experiments tunes feedback strength and changes the dynamic behaviour of the output of the synthetic transcriptional circuit with degronLOCKR feedback. Dynamic measurements of pZ3-Venus-cODC using automated flow cytometry for the synthetic-feedback strain with various combinations of feedback promoter strength and key length and no-feedback strain (pREV1-key-CFP-NLS), after induction with 3.13 nM progesterone and 7.5 nM oestradiol at 0 h. The lines represent a moving average taken over three data points and the points represent the mean ± s.d. of three biological replicates.

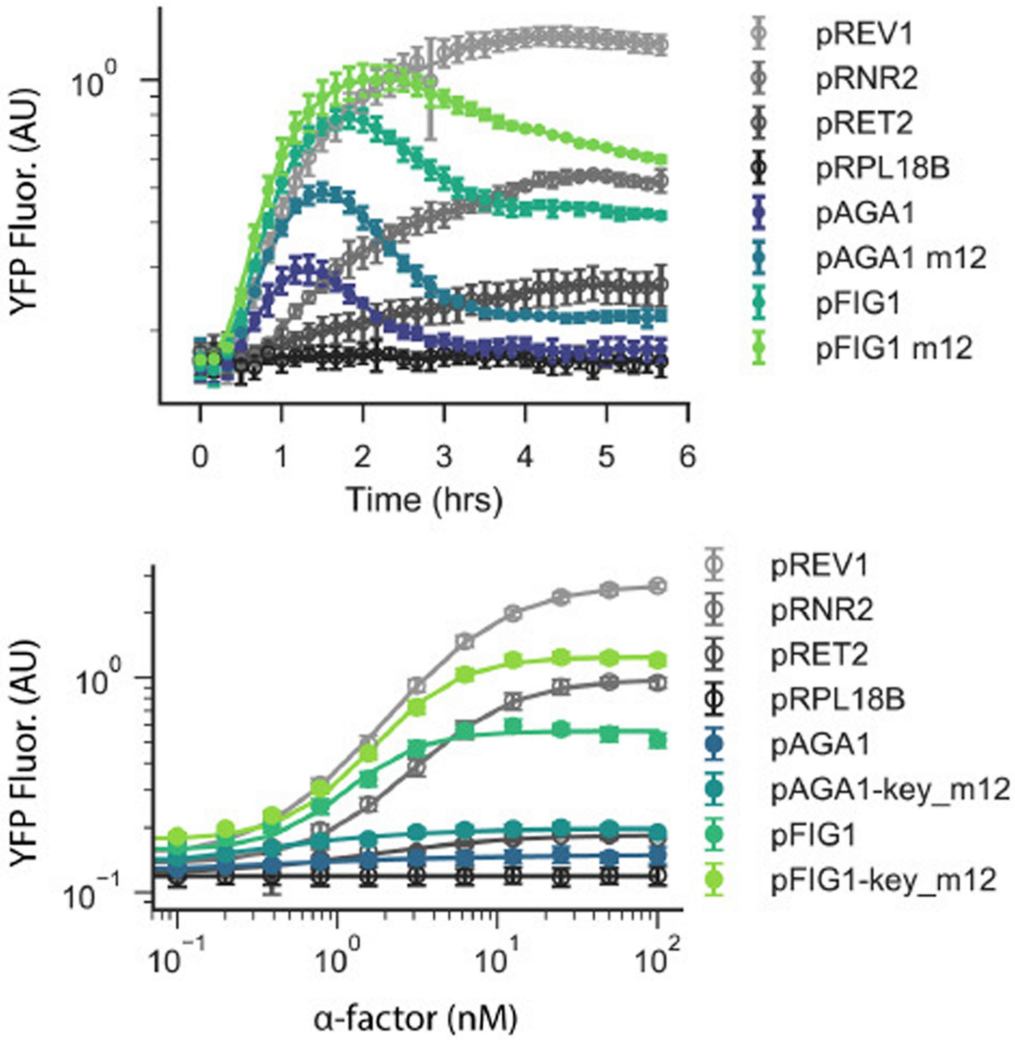

Extended Data Fig. 10 | Combinatorial tuning of synthetic negative feedback in the mating pathway. Top, dynamic measurements of pAGA1-YFP-cODC output for various feedback and no-feedback (*REV1*, *RNR2*, *RET2* and *RPL18B* promoter) strains with Ste12 fused to degronSwitch, after stimulation with 25 nM α-factor. The lines represent a moving average taken over three flow cytometry data points and the points represent the mean ± s.d. of three biological replicates. Bottom, α-factor dose–response of feedback strains versus no-feedback (*REV1*, *RNR2*, *RET2* and *RPL18B* promoter) strains. YFP fluorescence was measured using flow cytometry four hours after induction with α-factor. Points represent mean ± s.d. of three biological replicates. Lines are a Hill function fit to the data.

nature research

Corresponding author(s): Dr. Hana El-Samad

Reporting Summary

Nature Research wishes to improve the reproducibility of the work that we publish. This form provides structure for consistency and transparency in reporting. For further information on Nature Research policies, see Authors & Referees and the Editorial Policy Checklist.

Statistical parameters

When statistical analyses are reported, confirm that the following items are present in the relevant location (e.g. figure legend, table legend, main text, or Methods section).

n/a	Confirmed	
☐	☒	The exact sample size (*n*) for each experimental group/condition, given as a discrete number and unit of measurement
☐	☒	An indication of whether measurements were taken from distinct samples or whether the same sample was measured repeatedly
☐	☒	The statistical test(s) used AND whether they are one- or two-sided *Only common tests should be described solely by name; describe more complex techniques in the Methods section.*
☒	☐	A description of all covariates tested
☒	☐	A description of any assumptions or corrections, such as tests of normality and adjustment for multiple comparisons
☐	☒	A full description of the statistics including central tendency (e.g. means) or other basic estimates (e.g. regression coefficient) AND variation (e.g. standard deviation) or associated estimates of uncertainty (e.g. confidence intervals)
☐	☒	For null hypothesis testing, the test statistic (e.g. *F*, *t*, *r*) with confidence intervals, effect sizes, degrees of freedom and *P* value noted *Give P values as exact values whenever suitable.*
☒	☐	For Bayesian analysis, information on the choice of priors and Markov chain Monte Carlo settings
☒	☐	For hierarchical and complex designs, identification of the appropriate level for tests and full reporting of outcomes
☒	☐	Estimates of effect sizes (e.g. Cohen's *d*, Pearson's *r*), indicating how they were calculated
☐	☒	Clearly defined error bars *State explicitly what error bars represent (e.g. SD, SE, CI)*

Our web collection on statistics for biologists may be useful.

Software and code

Policy information about availability of computer code

Data collection	Flow cytometry data was collected using a combination of BD FACS Diva v6.1.3 and custom software written in LabView 2013
Data analysis	All analysis of data was performed using the FlowCytometryTools v0.5.0 and SciPy v1.1.0 package in Python 2.7.

For manuscripts utilizing custom algorithms or software that are central to the research but not yet described in published literature, software must be made available to editors/reviewers upon request. We strongly encourage code deposition in a community repository (e.g. GitHub). See the Nature Research guidelines for submitting code & software for further information.

Data

Policy information about availability of data

All manuscripts must include a data availability statement. This statement should provide the following information, where applicable:

- Accession codes, unique identifiers, or web links for publicly available datasets
- A list of figures that have associated raw data
- A description of any restrictions on data availability

The authors declare that all data supporting the findings of this study are available within the paper (and its Supplementary Information files), but original data that supports the findings are available from the corresponding authors upon reasonable request. Plasmids encoding the synthetic controller and process are available from Addgene (plasmids 127164 and 127165).

Field-specific reporting

Please select the best fit for your research. If you are not sure, read the appropriate sections before making your selection.

☒ Life sciences ☐ Behavioural & social sciences ☐ Ecological, evolutionary & environmental sciences

For a reference copy of the document with all sections, see nature.com/authors/policies/ReportingSummary-flat.pdf

Life sciences study design

All studies must disclose on these points even when the disclosure is negative.

Sample size	No sample size calculation was performed. Sample size of n=3 was deemed sufficient because no significant difference was observed between biological replicates
Data exclusions	No data was excluded
Replication	All experimental findings were replicated successfully using biological replicates on different days
Randomization	Randomization was not performed because genetically identical samples were used
Blinding	Blinding was not performed because experiments were carried out by individual researchers

Reporting for specific materials, systems and methods

Materials & experimental systems

n/a	Involved in the study
☐	☒ Unique biological materials
☒	☐ Antibodies
☒	☐ Eukaryotic cell lines
☒	☐ Palaeontology
☒	☐ Animals and other organisms
☒	☐ Human research participants

Methods

n/a	Involved in the study
☒	☐ ChIP-seq
☐	☒ Flow cytometry
☒	☐ MRI-based neuroimaging

Unique biological materials

Policy information about availability of materials

Obtaining unique materials	The unique materials (plasmids) that support the findings of this study are available from the corresponding authors upon reasonable request.

Flow Cytometry

Plots

Confirm that:

☒ The axis labels state the marker and fluorochrome used (e.g. CD4-FITC).

☒ The axis scales are clearly visible. Include numbers along axes only for bottom left plot of group (a 'group' is an analysis of identical markers).

☒ All plots are contour plots with outliers or pseudocolor plots.

☒ A numerical value for number of cells or percentage (with statistics) is provided.

Methodology

Sample preparation	Cells were grown in yeast media and diluted in TE solution to obtain an appropriate density or flowed directly into the instrument
Instrument	BD LSR II

Software	BD FACS Diva was used to collect data and analysis was performed using the FlowCytometryTools package in Python 2.7. Gating strategy was illustrated using FlowJo Version 10
Cell population abundance	Relevant cell fractions were above 90% for all samples
Gating strategy	Debris was removed by thresholding on SSC-H > 1000 and FITC-H > 10

☒ Tick this box to confirm that a figure exemplifying the gating strategy is provided in the Supplementary Information.